

The Selective and Sequential Aminolysis of Benzotrifuranone: A Synergism of Electronic Effects and a Ring Strain Gradient

Matthew B. Baker, Renan B. Ferreira, Jonathan Tasseroul, Andrew J.
Lampkins, Alexandre Al Abbas, Khalil A. Abboud, and Ronald K Castellano

J. Org. Chem., **Just Accepted Manuscript** • DOI: 10.1021/acs.joc.6b01867 • Publication Date (Web): 31 Aug 2016

Downloaded from <http://pubs.acs.org> on September 2, 2016

Just Accepted

“Just Accepted” manuscripts have been peer-reviewed and accepted for publication. They are posted online prior to technical editing, formatting for publication and author proofing. The American Chemical Society provides “Just Accepted” as a free service to the research community to expedite the dissemination of scientific material as soon as possible after acceptance. “Just Accepted” manuscripts appear in full in PDF format accompanied by an HTML abstract. “Just Accepted” manuscripts have been fully peer reviewed, but should not be considered the official version of record. They are accessible to all readers and citable by the Digital Object Identifier (DOI®). “Just Accepted” is an optional service offered to authors. Therefore, the “Just Accepted” Web site may not include all articles that will be published in the journal. After a manuscript is technically edited and formatted, it will be removed from the “Just Accepted” Web site and published as an ASAP article. Note that technical editing may introduce minor changes to the manuscript text and/or graphics which could affect content, and all legal disclaimers and ethical guidelines that apply to the journal pertain. ACS cannot be held responsible for errors or consequences arising from the use of information contained in these “Just Accepted” manuscripts.



The Selective and Sequential Aminolysis of Benzotrifuranone: A Synergism of Electronic Effects and a Ring Strain Gradient

Matthew B. Baker,[†] Renan B. Ferreira, Jonathan Tasseroul, Andrew J. Lampkins, Alexandre Al Abbas, Khalil A. Abboud, and Ronald K. Castellano*

Department of Chemistry, University of Florida, P.O. Box 117200, Gainesville, Florida 32611, United States

KEYWORDS: *isodesmic, kinetics, multifunctionalization, ring strain, selectivity*

ABSTRACT: Benzotrifuranone (**BTF**), bearing three symmetry-equivalent lactone rings, is unique in its ability to undergo highly selective and sequential aminolysis reactions in one-pot to afford multifunctionalized molecules (> 80% overall yield). New insight into this behavior is presented through kinetics measurements (by stopped-flow IR spectroscopy), X-ray crystal structure analysis, quantum chemical calculations, and comparison of **BTF** to other benzoate esters, including its ring expanded congener benzotripyranone (**BTP**). While the structure-property investigation confirms stepwise electronic/inductive lactone deactivation for both **BTF** and **BTP**, the unusually fast and selective aminolysis of **BTF** is only fully explained through synergistic ring strain effects. Experimental signatures of the significant ring strain of **BTF** (~ 28 kcal mol⁻¹ based on DFT calculations vs. 17 kcal mol⁻¹ for **BTP**) include its high lactone carbonyl stretching energy (1821 cm⁻¹ in acetonitrile vs. 1777 cm⁻¹ for **BTP**) and bond length alternation within its benzenoid ring. While ring strain is relieved upon the sequential aminolysis of both **BTF** and **BTP**, it is only for the former that a ring strain gradient is established that contributes to the stepwise aminolysis rate differences and enhanced selectivity. The work shows how a combination of electronic effects and ring strain can underpin the design of small molecules capable of stepwise functionalization, of which there are notably few examples.

INTRODUCTION

Synthetic methodology to rapidly and efficiently prepare multifunctional molecules continues to leverage discoveries in disciplines spanning materials science and chemical biology. Particularly attractive are protocols that provide access to complex targets through a series of reactions in a single pot, as they potentially reduce purification costs, eliminate waste, and lend themselves to diversity-oriented synthesis.¹ Excellent progress has been made to develop one-pot domino and multi-component reactions along these lines.² An alternative approach to discrete multifunctional architectures is exemplified by the chemistry of cyanuric chloride (**CC**)³ and its congeners (Figure 1a), wherein a highly symmetrical scaffold is efficiently desymmetrized, in one pot, through sequential substitution reactions across a convenient temperature range.⁴ As the paradigmatic framework displaying this reactivity profile, **CC** has facilitated access to diverse multifunctional targets for applications across the biological,⁵ supramolecular,⁶ synthetic,⁷ and materials sciences.⁸

The paucity of available scaffolds akin to **CC** speaks to the stringent kinetics requirements for a molecule with even three symmetry equivalent reactive sites to undergo synthetically useful stepwise functionalization. Given identical rates of reaction between any of sites A, A', or A'' with reagent site B (i.e., $k_{AB} = k_{A'B} = k_{A''B}$), a simple mathematical model (see the SI for details) predicts a paltry 44% maximum yield of the singly functionalized product and an abysmal start to the synthesis of a fully differentiated target (Figure 1b). An ideal system establishes a reactivity gradient (i.e., $k_{AB} \gg k_{A'B} \gg k_{A''B}$) and allows (i) efficient conversion of the starting material

to the mono-, di-, and trifunctionalized products provided reagent stoichiometric control and (ii) the sequential introduction of up to three different reagents. To the best of our knowledge, scaffolds fitting this reactivity paradigm have yet to be targets of systematic mechanistic/kinetic investigation,⁹ and therefore de novo design.

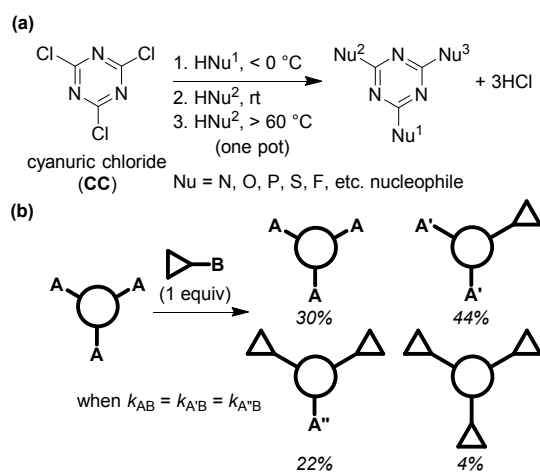
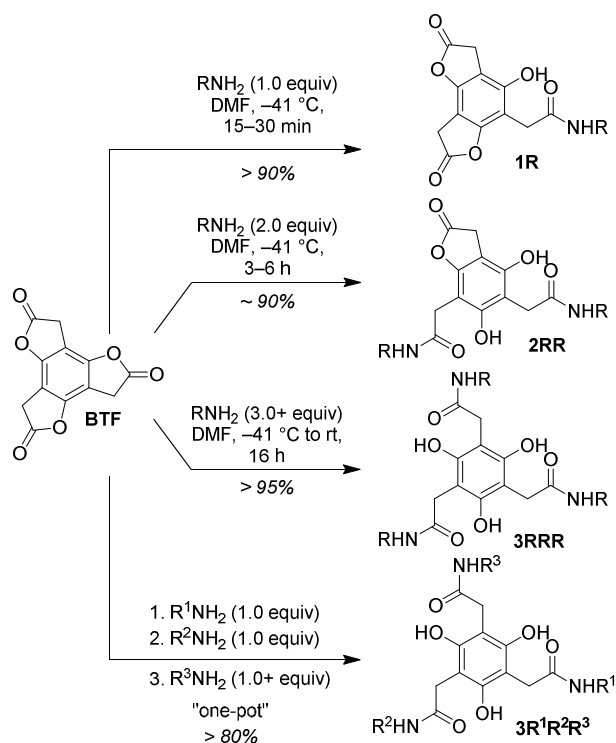


Figure 1. Outcomes for functionalization of a molecule bearing three symmetry equivalent reactive positions. (a) Efficient one-pot sequential multifunctionalization, exemplified by the chemistry of cyanuric chloride (**CC**), requires establishment of a reactivity (kinetic) gradient. (b) A statistical product mixture (percentages shown are from mathematical modeling) results if the reaction rates between reagent site B and positions A, A', and A'' are identical (assuming an irreversible reaction that goes to completion).

Scheme 1. Summary of Aminolysis Behavior of Benzotri-furanone (BTF)^a

^aSummary of **BTF** aminolysis reactivity from ref. 10. Yields shown are representative and determined from either ¹H NMR (**1R**, **2RR**) or isolation (**3RRR**, **3R¹R²R³**).

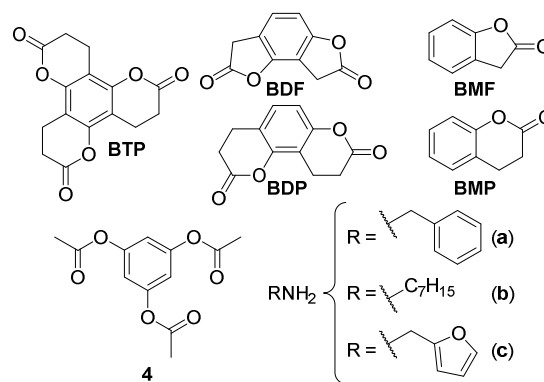
We recently reported¹⁰ that benzotri-furanone (**BTF**)¹¹ (Scheme 1), a C_{3h}-symmetrical trilactone, is unusually suited for multifunctionalization through sequential aminolysis reactions. The platform affords rapid and efficient access to mono- (e.g., **1R**), di- (e.g., **2RR**), and trifunctionalized (e.g., **3RRR**) targets provided routine control of temperature and amine reagent stoichiometry, and lends itself to the one-pot synthesis of multifunctionalized phloroglucinol, **3** (e.g., **3R¹R²R³**), from **BTF** in good yield (> 80%) and a single day.

We initially proposed a primarily electronic/inductive argument (given the stepwise substituent changes occurring on the central benzenoid ring) to rationalize the kinetic deactivation observed upon successive aminolysis of **BTF**. In this paper, we report a more comprehensive understanding of the aminolysis behavior of **BTF** through kinetics measurements, X-ray crystal structure analysis, and quantum chemical calculations. Included is comparison of **BTF** to various benzoate esters, such as a ring expanded congener, benzotripyranone (**BTP**) (Chart 1). Notably, our structure-property investigation exposes a ring strain gradient as a component of the sequential aminolysis behavior observed for **BTF**. While singular strain elements are appreciated as useful promoters of chemical reactions,¹² this study shows that *energetically coupled* strain-release events can afford stepwise reactivity and can serve as the basis for sequential molecular functionalization.

RESULTS AND DISCUSSION

Numbering Convention. Throughout the paper, **BTF** and **BTP** aminolysis products are first numbered based on their parent structure. Letters after the numbers designate the number, type, and sequence of amines (Chart 1) used to form the

Chart 1. Benzoate ester derivatives and amines used in this work.



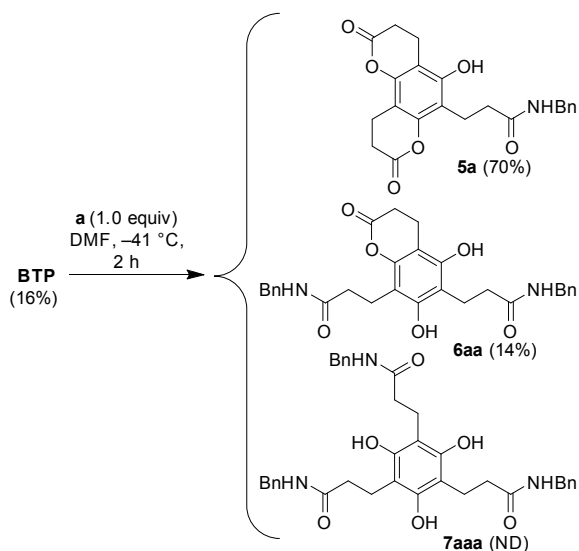
aminolysis product. For example, compound **1** (Scheme 1) produced by aminolysis of **BTF** with one equivalent of amine **a** will be denoted **1a**, while **2** produced from **BTF** using two equivalents of amine **a** will be denoted **2aa**, and so on.

Benzoate Esters Used in this Work (Chart 1). **BTF**,¹¹ **BMF** (2-coumaranone),¹¹ and **4** (phloroglucinol triacetate) were synthesized following literature precedent (see the SI for details); **BMP** (3,4-dihydrocoumarin) was purchased commercially. The synthesis of benzotripyranone **BTP**, a new compound, could be completed quantitatively through acid-catalyzed intramolecular transesterification of known triisopropyl 3,3',3''-(2,4,6-trihydroxybenzene-1,3,5-triyl)tripropionate (which is available in six steps¹³ from 1,3,5-trimethoxybenzene). Noted previously,¹¹ attempts to prepare **BTF** using "reversible" (e.g., Lewis and Bronsted acid catalyzed) lactonization conditions were plagued by the formation of stable, partially cyclized intermediates. The observation that **BTP** is formed quantitatively under the same conditions speaks to its relative thermodynamic stability. The remaining compounds shown in Chart 1, **BDF** and **BDP**, have been used exclusively in calculations (vide infra).

General Aminolysis Behavior: BTF vs. BTP. **BTP**, like **BTF**, forms a dilactone (**5a**) as the major product upon reaction with one equivalent of an aliphatic amine like benzylamine (**a**) (Scheme 2). The reaction, however, under conditions identical to **BTF** aminolysis, is *considerably slower and lower yielding* with respect to the monoaminolysis adduct (i.e., the reaction is less selective). HPLC analysis (see Figure S1) of the crude reaction after 2 h (at -41 °C in DMF), for example, reveals a mixture of **BTP** (16%), **5a** (70%), and **6aa** (14%) (and no detectable **7aaa**). The conversion to **5a**, nonetheless, exceeds predictions given equivalent lactone reactivity (44%). Similar results are found (not shown in Scheme 2) upon reaction of **BTP** with *n*-heptylamine (**b**) (where **5b** is prepared in 71% isolated yield). Treatment of **BTP** with *two equivalents* of **a** or **b** provides the corresponding monolactones (**6aa** and **6bb**, respectively) in ~ 60% yield, again exceeding the 50% predicted from equally reactive lactones. Phloroglucinol **7** can be prepared essentially quantitatively with an excess of amine (and warming to room temperature overnight) as shown through the preparation of **7bbb** (see the SI for details). These synthetic experiments give the first indication that a simple inductive argument is not sufficient to explain the high selectivity of **BTF** aminolysis.

Aminolysis Rate Constants: Determination and Caveats. The aminolysis of simple phenyl acetates in polar aprotic

Scheme 2. Representative Aminolysis of Benzotripyranone (BTP)^a



^aPercentages shown in parentheses are relative amounts of **BTP**, **5a**, **6aa**, and **7aaa** based on HPLC analysis of the crude reaction mixture after 2 h. The *isolated yield* of **5a**, in a separate preparation under similar conditions, is comparable (see the SI for details). ND = not detected

solvents has been extensively studied from both an experimental¹⁴ and a theoretical point of view.^{14b,15} Typically, second-order kinetics (first order in amine and ester) are observed,^{14b-e} although some studies have presented evidence for a third order process.^{14f,16} In light of this data, pseudo-first-order conditions generally using an excess of amine, *n*-heptylamine (**b**), were established for determination of aminolysis rate constants for **BTF** and **BTP**, their products, and selected simpler systems (Chart 1). Due to the rapid aminolysis of **BTF**, the aminolysis rates were measured in all cases by stopped-flow FT-IR spectroscopy (Table 1 and Table S1), approximated by the rate of disappearance of the relevant lactone C=O absorptions (Figure 2a and Figure S2). All measurements were made in acetonitrile, a solvent which provided a good window of visibility (1750–1800 cm⁻¹) at 24.0 ± 0.2 °C.

The *n*-heptylaminolysis of **BTP** (Figure 2b) is illustrative. An absorption difference plot ($A-A_0$) over the first minute accentuates the change in the **BTP** C=O absorption at 1776 cm⁻¹ (and accompanying increase in amide I (C=O) absorption, ~1640 cm⁻¹, not shown). While data used for determination of k_{obs} was limited to the early (and linear) portion of the pseudo-first-order rate plot, it is critical to appreciate that the absorption maxima for the lactones along the aminolysis pathway for **BTP** are only modestly separated ($\Delta\nu_{\text{max}} \sim 5 \text{ cm}^{-1}$)—such is also the case for **BTF** and **4**. In this example, contaminating the diminishing **BTP** absorption at 1776 cm⁻¹ are the increasing lactone C=O absorptions for **5b** at ~1773 cm⁻¹. Given the complication, the observed lactone disappearance of **BTP** has been corrected for the appearance of the lactones of **BDP** (using the molar absorptivity at 1776 cm⁻¹, see SI for details). Therefore, this A_{corr} accurately reflects the concentration of the molecular species, and the k_{obs} is the real rate of disappearance, in this case, of **BTP**. Identical approaches were utilized for all molecules that have overlapping product peaks

(i.e. **BTF**, **1b**, **5b**, and **4**) Linear regression analysis (adjusted R -squared = 0.999) of the $\ln(A_{\text{corr}})$ versus t plot (inset)

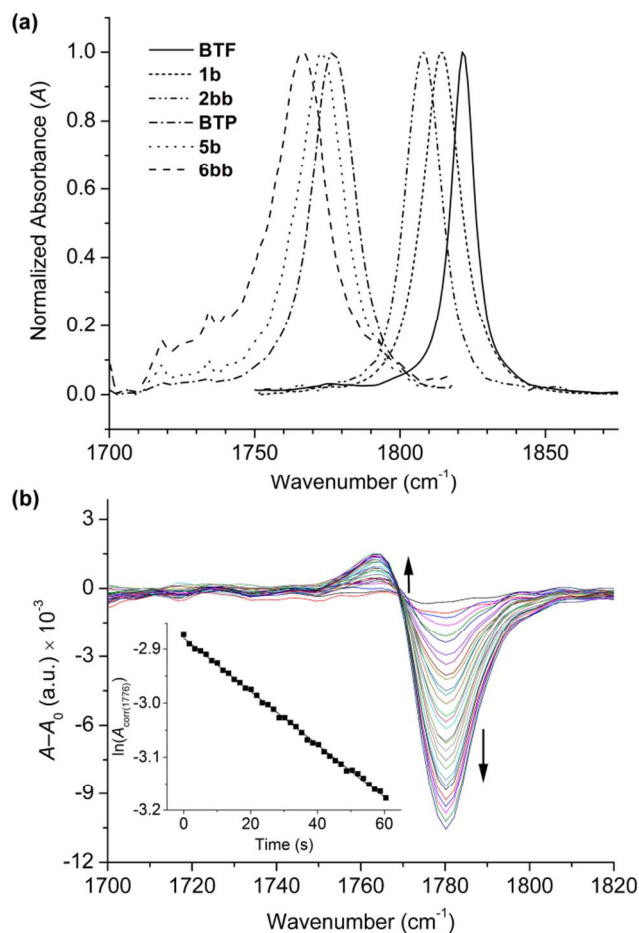


Figure 2. (a) Normalized IR absorption spectra (lactone C=O region) of **BTF**, **BTP**, and their *n*-heptylaminolysis products recorded as dilute ($\sim 5 \times 10^{-3}$ M) solutions in acetonitrile. (b) Representative *n*-heptylaminolysis data for **BTP** in acetonitrile at 24 °C ($[\text{BTP}] = 2.55 \text{ mM}$; $[\text{b}] = 58.8 \text{ mM}$). IR difference spectra ($A-A_0$; arrows show evolution with time) and the associated pseudo-first order kinetic plot are shown. Results of linear regression analysis: $k_{\text{obs}} = 0.00488 \text{ s}^{-1}$; adjusted R -squared = 0.999. See the SI for additional plots and full data analysis.

confirms pseudo-first-order kinetics and offers a slope (k_{obs}) of 0.00488 s^{-1} . The standard error in the rate based on six replicate runs (Table S1) is ± 0.4% (see the SI for details). Representative kinetic plots for all of the relevant compounds in this work are shown in Figures S3–S5.

Finally, conversion to apparent second-order rate constants (k) comes through $k_{\text{obs}}/[\text{amine}]$. For **BTP**, **BTF**, **1b**, **4**, and **5b**, the rate constants have been further statistically corrected (by the number of similarly reactive carbonyl groups in the molecules) to facilitate comparison on a per lactone basis (k_{lac}). Assumed, and borne out qualitatively in previous studies,¹⁰ is that the two different lactones within **1b** and within **5b** react comparably.

Aminolysis Kinetics: General Observations. Immediately apparent from the kinetics data (Table 1) is the extremely rapid monoaminolysis of **BTF** at room temperature ($k = 14.6 \text{ M}^{-1} \text{ s}^{-1}$). The aminolysis rate ($k_{\text{lac(BTF)}}$, on a per-ester basis) is *two orders of magnitude* faster than six-membered ring congener

BTP, 22 times faster than *p*-nitrophenyl acetate (a conventional “activated ester”) under comparable conditions,^{14b} and

Table 1. Aminolysis Rate Constants^a

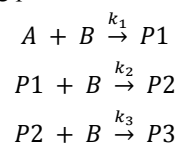
compound	k_{lac} ($\text{M}^{-1} \text{s}^{-1}$), [k] ^b	$k_{\text{lac,rel}}$, [k_{rel}] ^c
BTF	4.87±0.06 [14.6±0.2]	934 [2802]
1b	0.0890±0.0050 [0.178±0.010]	17 [34]
2bb	0.0126±0.0014	2.4
BTP	0.0277±0.0001 [0.0830±0.0003]	5.3 [16]
5b	0.0295±0.0002 [0.0590±0.0003]	5.7 [11]
6bb	0.00682±0.00026	1.3
BMF	0.0128±0.0003	2.5
BMP	0.00521±0.00019	1.0
4	0.00230±0.00007 [0.00691±0.00022]	0.4 [1.3]

^aExperimental rate constants determined for *n*-heptylaminolysis under pseudo-first-order conditions at 24.0 ± 0.2 °C in acetonitrile. See the SI for details. ^bApparent second-order rate constants. k_{lac} rates have been statistically corrected for the number of reactive carbonyl groups. Assumed is that the two different lactones within **1b** and within **5b** reacted comparably. The standard error shown is derived from 3–6 replicate runs. k rates in brackets have not been statistically corrected and are obtained directly as $k_{\text{obs(average)}}/[n\text{-heptylamine}]$. ^cRelative aminolysis rates with and without statistical correction for the number of reactive carbonyl groups.

2,300 times faster than acyclic triacetate **4**. Also apparent is the reactivity gradient established *within* the **BTF** and **BTP** families, where the lactone rate differences along the aminolysis pathway are more disparate in the former ($k_{\text{lac(BTF)}}:k_{\text{lac(1b)}}:k_{\text{lac(2bb)}} = 390:7.1:1.0$ versus $k_{\text{lac(BTP)}}:k_{\text{lac(5b)}}:k_{\text{lac(6bb)}} = 4.1:4.3:1.0$). The disparity translates directly into the sequential aminolysis selectivity differences observed for the two systems read out from product yields (i.e., Schemes 1 and 2). The difference in aminolysis rate for **BMF** and **BMP** ($k_{\text{lac(BMF)}}:k_{\text{lac(BMP)}} = 2.5:1.0$) speaks to an intrinsic difference between the bicyclic rings (that contrasts with their alkaline hydrolysis profile where $k_{\text{lac(BMF)}}:k_{\text{lac(BMP)}} = 1.0:9.7^{17}$). While the difference is mirrored in $k_{\text{lac(2bb)}}:k_{\text{lac(6bb)}} = 1.8:1.0$, a departure in the ratio is noted as additional rings are added ($k_{\text{lac(BTF)}}:k_{\text{lac(BTP)}} = 180:1.0$ and $k_{\text{lac(1b)}}:k_{\text{lac(5b)}} = 3.0:1.0$) in part as a consequence of cumulative ring-based (e.g., strain) effects (vide infra).

Aminolysis Kinetics: Relationship to Aminolysis Product Yields. The rate data shown in Table 1 should allow estimation of the aminolysis product distribution expected upon treatment of either **BTF** or **BTP** with one equivalent of *n*-heptylamine **b**, and therefore a separate way to evaluate their consistency. Of note, this kinetic analysis is based on the statistically uncorrected rates (k) since we are evaluating the selective production of chemical entities and not comparing functional groups as above. Aminolysis of **BTF/BTP** occurs through a series of three irreversible consecutive reactions and is therefore governed by the general kinetic expressions de-

rived for “triple consecutive competitive systems”.¹⁸ Since an analogous experimental kinetic analysis of **CC** has yet to be done, the work of Friedman and White¹⁹ that has specifically considered the following consecutive reaction sequence provides a generic starting point:



In the specific cases described in this work, **A** is either **BTF** or **BTP**, **B** is an amine nucleophile (e.g., **b**), **P1** is a dilactone (i.e., **1** or **5**), **P2** is a monolactone (i.e., **2** or **6**), and **P3** is a phloroglucinol (i.e., **3** or **7**).

Modification of the Friedman and White analysis to assume complete conversion of the amine and a 1:1 stoichiometry of reactants (i.e., $[A]_0 = [B]_0$), an additional mass balance constraint can be introduced, and a relationship between rate ratios (or *selectivity factors*, k_1/k_i) and the final product ratios can be derived (see the SI for details). The derivation allows the prediction of product ratios within a sequence given the rate constants, or estimation of the ratio of rate constants based on the product ratios of an experimental result. When $k_1 = k_2 = k_3$ (i.e., where $k_1/k_2 = k_1/k_3 = 1$) a statistical product distribution results from the analysis with 36% A, 37% P1, 19% P2, and 8.4% P3 (Table S2). Satisfyingly, this distribution is *essentially identical* to the distribution determined by statistical modeling reported in our previous work¹⁸ and discussed in the SI. Illustrative for this work, if one assumes the statistically corrected k_{lac} rates are equal (i.e., $k_1 = \frac{3}{2}k_2 = 3k_3$) then the product distribution becomes 30% A, 44% P1, 22% P2, and 4% P3. At the other extreme, to achieve 98% P1 (dilactone), k_1/k_2 must approach 500. If one defines a synthetically acceptable yield as 90%, the demands on the system are greatly reduced, and k_1/k_2 need only be ~ 50 .

Use of this analysis to comport the product distributions observed for **BTF** (Scheme 1) and now **BTP** (Scheme 2) requires assuming the selectivity factors: 1) in acetonitrile and DMF are similar and 2) can be faithfully extrapolated to other temperatures. Speaking to the former, the *n*-heptylaminolysis of **BTF** in acetonitrile at -15 °C shows $\sim 95\%$ conversion to **1b**, comparable to the result obtained at -41 °C in DMF (data not shown). The Arrhenius equation then allows selectivities at -41 °C (233K) to be estimated, with some assumptions, from those obtained at 297 K (Table 2 and Table S3). Naturally, the selectivities increase at lower temperatures. Most importantly, the predicted product distributions match well with those found experimentally (Schemes 1 and 2). To wit, the nearly quantitative experimental conversion of **BTF** to **1b** at low temperature is consistent with the 97% yield predicted on the basis of selectivity factors that exceed 100 (Table 2, entry 1). The much smaller selectivity factors associated with **BTP** aminolysis predict a marginally better than statistical product outcome; the experimental conversion to **5b** (70%) is only reasonably approximated by the 45% yield anticipated on the basis of its sequential reaction rates (Table 2, entry 2). This result suggests that the kinetic differences between the aminolysis of **BTP** and **5a** in DMF are larger than those measured in acetonitrile. Based on the experimental yield of **5b**, one would expect a rate ratio ($k_{\text{BTP}}/k_{\text{5b}}$) of ~ 10 between **BTP** and **5b** (see SI for expected outcomes based on rate ratios).

Table 2. Predicted, Observed, and Statistical Aminolysis Product Outcomes for BTF and BTP^a

substrate	k_1/k_2 (297K) ^b [k_1/k_2 , 233K] ^c	k_1/k_3 (297K) ^b [k_1/k_3 , 233K] ^c	A (% , predicted) ^d [A, % , observed, ^e statistical ^f]	P1 (% , predicted) ^d [P1, % , observed, ^e statistical ^f]	P2 (% , predicted) ^d [P2, % , observed, ^e statistical ^f]	P3 (% , predicted) ^d [P3, % , observed, ^e statistical ^f]
BTF	82.0 [275]	1160 [8050]	1.2 [< 1 , ^g 36]	97.5 [> 96 , ^g 37]	1.2 [< 3 , ^g 19]	0.1 [ND, ^g 8]
BTP	1.41 [1.54]	12.2 [24.2]	27.8 [16, 36]	45.0 [70, 37]	26.7 [14, 19]	0.5 [ND, 8]

^aProduct ratios assuming reaction of 1 equiv of starting material (A, **BTF** or **BTP**) and 1 equiv of *n*-heptylamine (B). ^bRatio of appropriate Table 1 rate constants (e.g. $k_{\text{BTF}}/k_{\text{1b}}$, selectivity factors) based on *n*-heptylaminolysis at 297 K in acetonitrile. ^cRate ratios extrapolated to 233 K based on Arrhenius analysis. ^dStarting material and product percentages predicted from 233 K rate ratios. ^eObserved (experimental) product percentages for *n*-heptylaminolysis in DMF at 233 K (¹H NMR yields for the first two entries; isolated yields for the last two entries). ^fStarting material and product percentages predicted when $k_1/k_2 = k_1/k_3 = 1$. ^gData taken from ref. [10]. ND = not detected.

Table 3. Experimentally- and Computationally-Derived Aminolysis Reactivity Indicators^a

entry	parameter	BTF	1b	2bb	BTP	5b	6bb	BMF	BMP	4
1	$\delta_{\text{C=O(lactone)}}$ (ppm) ^b	173.4 ^c	174.2, 173.9 ^c	174.6 ^c	167.3	168.0, 167.9	168.7	174.4 ^d	168.3	168.7
2	$\nu_{\text{C=O(lactone)}}$ (cm ⁻¹) ^e	1821	1815	1808	1777	1773	1766	1812	1772	1774
3	C=O (Å)	1.188 ^{c,f} [1.192(3)] ^{d,f}	1.190, 1.191 ^c [1.192(2), 1.199(2)] ^g	1.193 ^c	1.196 ^f [1.201(2)] ^{f,g}	1.198, 1.199 [1.204(1), 1.205(1)] ^g	1.200	1.191	1.198	1.199 ^f [1.197(4)] ^{f,h}
4	O–C(O) (Å)	1.401 ^{c,f} [1.388(3)] ^{d,f}	1.394, 1.401 ^c [1.379 (19), 1.396(19)] ^g	1.394 ^c	1.383 ^f [1.379(17)] ^{f,g}	1.378, 1.379 [1.366(13), 1.367(13)] ^g	1.373	1.388	1.375	1.375 ^f [1.366(4)] ^{f,h}
5	π^* occ. (C=O) ⁱ	0.180 ^{c,f}	0.183, 0.187 ^c	0.190 ^c	0.181 ^f	0.187, 0.188	0.193	0.192	0.189	0.196
6	ω (eV) ^j	1.73 ^c	1.38 ^c	1.10 ^c	1.59	1.25	1.00	1.43	1.31	1.33
7	LUMO (eV)	-1.59 ^c	-1.14 ^c	-0.74 ^c	-1.41	-0.99	-0.65	-1.20	-0.98	-0.99
8	V_{C} (au) ^k	-14.610 ^f	-14.620, – 14.626	– 14.636	-14.621 ^f	-14.636, – 14.632	– 14.646	– 14.630	– 14.634	-14.630

^aData in entries 1 and 2 are derived from experimental data obtained for the specifically indicated compounds. Data for the remaining entries are derived from quantum chemical calculations (at the B3LYP/6-311++G** level) unless specified otherwise, also on the specifically indicated compounds, except for **1b**, **2bb**, **5b**, and **6bb** where the *n*-heptyl groups have been truncated to methyl groups. ^b¹³C NMR chemical shifts for the lactone carbonyl carbons (in DMSO-*d*₆). ^cData taken from ref. [10]. ^dData taken from ref. [11]. ^eIR carbonyl energies from acetonitrile solution (0.05–0.3 M). ^fAverage value for multiple carbonyl groups. ^gFrom X-ray crystallographic data reported in this work for **BTP**, **1c**, and **5a**. ^hFrom X-ray crystallographic data reported in ref. [20]. CSD code: DUJTIM. ⁱOccupancy of the lactone carbonyl π^* orbital from NBO population analysis. ^jCalculated global electrophilicity index. ^kElectrostatic potential at nuclei (EPN).

Origins of Sequential Aminolysis Reactivity: Electronic Effects. Even in the absence of a detailed aminolysis reaction mechanism (but assuming the same aminolysis mechanism for all of the compounds studied here), a Hammett-type analysis might predict sequential aminolysis reactivity for both the **BTF** and **BTP** systems given the substituent changes that occur at the central benzene ring along the reaction pathway. Each successive aminolysis reaction converts one –OC(=O)CH₂– substituent to a less electron withdrawing –OH substituent²¹ *meta* to the phenyl oxygen of a common lactone ring (–OH: $\sigma_1 = 0.33$, $\sigma_m = 0.12$; –OAc: $\sigma_1 = 0.42$, $\sigma_m = 0.39$ ²²). The increasingly downfield lactone carbonyl ¹³C NMR resonances (Table 3, entry 1) and lower $\nu_{\text{C=O}}$ wavenumbers (Figure 2a and Table 3, entry 2) from **BTF**→**1b**→**2bb** (and **BTP**→**5b**→**6bb**) are consistent with this increase of electron density at the benzene ring based on spectroscopic trends known for *meta*- and *para*-substituted phenyl acetates.^{14d,23} It

further follows that the rate of aminolysis should progressively decrease, again given similar behavior observed upon introduction of electron-donating substituents (R²) to phenyl acetates of the general structure *p*-R²PhOC(=O)R¹.^{14b,14c,14e,14f,15a,16,24}

While consideration of substituent changes does predict the reactivity trend, it does not appear to fully capture the differences in aminolysis rate either between **BTF** and **1b**, or between **BTF** and **BTP**. In both series, **BTF**→**1b**→**2bb**→**3bbb** and **BTP**→**5b**→**6bb**→**7bbb**, each aminolysis event reflects a $\Delta\sigma_m$ of ~ 0.3 and a $\Delta\sigma_1$ of ~ 0.1 (~OAc→OH). For the aminolysis of *p*-substituted phenyl acetates in CH₃CN (where $\rho = 3.3$, a value derived using $\log k/k_0 = \sigma_p\rho$ from experimental rate data^{14b}), a $\Delta\sigma_p$ of ~ 0.3 constitutes a ~ 10-fold rate change (or $k_1/k_2 \sim 10$). Not only does the **BTF** aminolysis sequence not subscribe to a linear rate progression, $k_{\text{lac(BTF)}}/k_{\text{lac(1b)}}$ is ~ 50. That $k_{\text{lac(BTF)}}:k_{\text{lac(BTP)}}$ equals 180:1.0 (vide supra) also sug-

gests that **BTF**, and perhaps **1b**, benefit from a boost in reactivity beyond statistical and electronic considerations. Worth noting, however, is that these two factors (steric effects notwithstanding) may sufficiently describe the rate differences observed along **BTP**→**5b**→**6bb**→**7bbb**.

Nonetheless, as described in our earlier work, a variety of computationally (DFT) derived reactivity descriptors nicely predict, on the basis of electronic structure, an aminolysis rate gradient as **BTF** > **1b** > **2bb**. The approach is extended here to **BTP**, **5b**, **6bb**, and selected model compounds (Table 3 and Tables S4 and S5). Low energy geometries for the new molecules have been obtained in the gas phase at the B3LYP/6-311++G** level, and frequency calculations have been performed to assign the structures as minima (details, including structural coordinates, are provided in the SI).

An increase in the lactone C=O (entry 3) and decrease in the O–C(O) (entry 4) bond lengths are readily apparent along **BTF**→**1b**→**2bb** and **BTP**→**5b**→**6bb** (consistent with the IR C=O stretch data, and mirrored in X-ray crystallographic data, vide infra). This data together with entries 1–2 and the increasing lactone carbonyl π^* occupancy values²⁵ (NBO population analysis,²⁶ entry 5) from **BTF**→**2** and **BTP**→**6** are consistent with greater delocalization of the phenolic oxygen electrons into the lactone carbonyl and decreased carbonyl electrophilicity. The reactivity trend is also mirrored by decreasing global electrophilicity values²⁷ (ω , entry 6), increasing LUMO energies (entry 7), and decreasing electrostatic potentials at nuclei (EPN)²⁸ (entry 8). The latter parameter was previously indicated to be the best electrostatic predictor of aminolysis rates in model phenyl acetates by Galabov, et al.^{14b}

Mostly all of these computationally determined reactivity descriptors speak to the stepwise decrease in reactivity within a series (i.e., **BTF** and **BTP**) while also supporting the increased reactivity of the **BTF** series as compared to the **BTP** series. The same experimental and theoretical reactivity descriptors do well to predict the increased aminolysis rate of model compound **BMF** versus **BMP** or **4**. We were not, however, able to more quantitatively correlate the experimentally-determined rate constants to the computed reactivity parameters in these systems.

Structural Confirmation and Reactivity Clues from X-ray Crystallography. Crystals suitable for X-ray diffraction could be obtained for **BTF**, **1c**, **BTP**, and **5a** (the crystal structure of **BTF** has been previously reported;¹¹ CSD code: MUDBIX); the solved structures are shown in Figure 3 and full crystallographic details can be found in the SI (Table S9). When comparing diagnostic bond lengths of the benzofuranones (**BTF** and **1c**) to the benzopyranones (**BTP** and **5a**) (Figure 3 and Table 3, entries 3 and 4), there is good agreement with computational data and the trends that emerge speak to differences in reactivity. The five-membered ring lactone structures are characterized by both shorter C=O (lactone) bond lengths (**BTF** average 1.194 Å, **1c** average 1.196 Å) and longer O–C=O bond lengths (**BTF** average 1.388 Å, **1c** average 1.388 Å) as compared to the six-membered ring lactones (average C=O: **BTP**, 1.201 Å; **5a**, 1.205 Å; average O–C=O: **BTP**, 1.378 Å; **5a**, 1.367 Å). The average C=O bond length also increases upon ring opening in each family (e.g., from **BTF** to **1c**; from **BTP** to **5a**). Of additional note, the lactone rings of **BTF** and **1c** are essentially coplanar with the central aromatic ring, while those of **BTP** and **5a** are significantly puckered. That this geometry difference could influ-

ence the extent of π -delocalization of the phenolic oxygen lone pair into the central benzene ring in each case is reflected in the shorter O–C_{aryl} bond length for **BTF** versus **BTP** (average O–C_{aryl}: **BTF**, 1.388 Å; **BTP**, 1.402 Å). Overall, it is a decrease in the carbonyl and O–C_{aryl} bond lengths and increase in the O–C=O bond lengths that parallels increased lactone aminolysis reactivity.

Also critically evident from the X-ray structural data are C–C bond length distortions imposed on the central benzene ring of **BTF**, but not **BTP**, as a consequence of the fused lactones. **BTF** reveals a bond length alternation (ΔR)²⁹ of 0.024 Å (0.021 Å averaged over two crystallographically independent molecules), comparable to tricyclobutabenzene,³⁰ where the benzene C–C bonds contained within the five-membered lactone rings are longer than those between the fused rings. **BTP** shows a negligible ΔR of 0.003 Å (Figure 3). The ΔR values are reproduced excellently by DFT calculations (see Table S6). The phenomenon of angle-strain induced bond alternation in especially threefold symmetric benzenoid systems is well-documented (and often times referred to as the Mills-Nixon effect).^{29–31} Consequently, it is reasonable to consider whether the deviations in core benzene structure between **BTF**, **BTP**, and their ring-opened aminolysis products speak to differences in strain and therefore reactivity (vide infra).

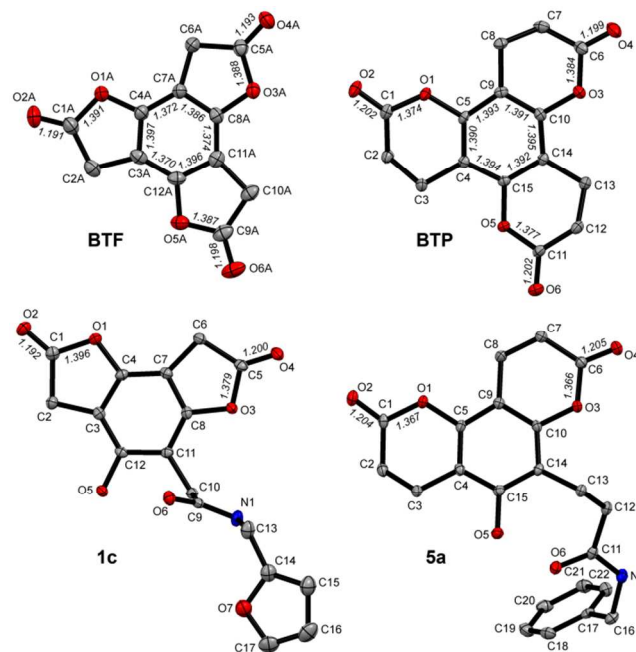


Figure 3. X-ray crystal structures of **BTF**, **BTP**, **1c**, and **5a**. Selected bond distances are shown in Å. Hydrogen atoms and solvent molecules have been omitted for clarity. Only one of the crystallographically independent molecules is shown for **BTF**. Thermal ellipsoids are drawn at the 50% probability level. Atom colors: blue = nitrogen; gray = carbon; red = oxygen. See the SI for additional plots and full data analysis.

Origins of Sequential Aminolysis Reactivity: Strain. In addition to the bond length alternation evident within the central benzene ring of **BTF**, the IR data shown in Figure 2/Table 3 is compelling with respect to diagnosing the unusual strain associated with this molecule. Ring strain, especially in cyclic lactones, has long been evaluated against the C=O stretch energy. Take, for example, the IR data (in CCl₄)³² for the classic

Table 4. Enthalpies of Formation for Parent Benzofuran Heterocycles from Homodesmotic Reactions and Estimation of Strain Enthalpies

	BTF	BTP	BDF	BDP	BMF	BMP
$\Delta_f H^\circ_{\text{gas-expt}}$	–	–	–	–	–51.1 ^b	–59.2 ^c
$\Delta_f H^\circ_{\text{gas-calcd}}^d$	–190.3	–214.1	–121.3	–136.6	–51.7	–58.3
$\Delta_f H^\circ_{\text{gas-GAV}}^e$	–218.1	–231.3	–138.8	–147.6	–59.5	–63.9
$\Delta_f H^\circ_{\text{gas-calcd}} - \Delta_f H^\circ_{\text{gas-GAV}}$ (“strain enthalpy”)	27.9	17.3	17.5	11.0	8.4	4.7
strain loss (BT→BD)	10.4	6.3	–	–	–	–
strain loss (BD→BM)	–	–	9.1	6.3	–	–

^aAll enthalpies or heats of formation have been determined in the gas phase at 298 K. All values in the table are in kcal mol^{–1}. GAV = strain-free group additivity value. ^b Ref. ³³. ^c Ref. ³⁴. ^d Determined from up to two different homodesmotic reactions and known $\Delta_f H^\circ_{\text{gas-expt}}$ values (see the SI for details). ^e Determined from strain-free group additivity values (see the SI for details).

molecular series of four-membered β -propiolactone ($\nu_{\text{C=O}}$ = 1818 cm^{–1}), five-membered γ -butyrolactone ($\nu_{\text{C=O}}$ = 1775 cm^{–1}), and six-membered δ -valerolactone ($\nu_{\text{C=O}}$ = 1740 cm^{–1}). The carbonyl stretching energy (in CH₃CN) for **BTF** ($\nu_{\text{C=O}}$ = 1821 cm^{–1}) exceeds that of β -propiolactone! Historical studies remind us to treat this IR data cautiously. To wit, the experimental (calorimetric) ring strain enthalpy³⁵ does not follow the IR trend as β -propiolactone (23 kcal mol^{–1}) > δ -valerolactone (9.5 kcal mol^{–1}) > γ -butyrolactone (7.7 kcal mol^{–1}), a result of the interplay between angle/torsional strain and stereoelectronic effects. The strain trend is mirrored in associated reaction rates and reversible polymerization capability.³⁶

A more relevant approach is to look at bicyclic benzolactones, where **BMF** (Chart 1) has been estimated to be (on the basis of solution-phase hydrolysis studies) ~1.2 kcal mol^{–1} more strained **BMP**.¹⁷ The data suggests that the $\nu_{\text{C=O}}$ values may follow the strain trend for these fused systems, and therefore be a reasonable predictor of, in this case, relative aminolysis reactivity. So, is **BTF** more “strained” than **BTP**, and is strain expected to be relieved (at least with respect to the heterocyclic core) upon aminolysis? To approach quantifying strain effects we performed a series of theoretical (DFT; B3LYP/6-31+G**) calculations to estimate the “strain energy” of the model heterocycles (Chart 1) that represent substructures of the species formed along the aminolysis pathways of both **BTF** and **BTP**. The results are given in Table 4 and relevant data is provided in Tables S7 and S8. To evaluate strain, theoretical heats of formation at 298 K ($\Delta_f H^\circ_{\text{gas-calcd}}$)—determined from appropriate homodesmotic reactions³⁷ (see the SI for the reactions used) involving experimental $\Delta_f H^\circ_{\text{gas}}$ values—were compared to values determined for hypothetical “unstrained” molecules (through strain-free group additivity values). That the approach is sound comes, in part, through the excellent agreement (within 2%) between the experimental and theoretical $\Delta_f H^\circ_{\text{gas}}$ values for **BMF** and **BDF** (Table 4). The trends in strain enthalpy values are consistent with the overall aminolysis rate behavior found for the individual **BTF** and **BTP** series. That is, $k_{\text{lac}}(\text{BTF}) > k_{\text{lac}}(\text{BDF}) > k_{\text{lac}}(\text{BTP}) \geq k_{\text{lac}}(\text{BDP})$ (on a per lactone basis) as strain (on a per lactone basis) decreases as **BTF** > **BDF** > **BTP** \geq **BDP**. Moreover, the strain loss difference in BT→BD between **BTF** and **BTP** (10.4 – 6.3 = 4.1 kcal mol^{–1}) is, admittedly fortuitously, in the ballpark of the activation energy difference (~ 3 kcal mol^{–1}) that corresponds to the 180-fold difference in experimental monoami-

nolysis rate between the compounds. More interesting is that the change in ring strain along the hypothetical reaction pathway **BTF**→**BDF**→**BMF** is not constant; the strain loss in the first step (10.4 kcal mol^{–1}) is greater than the second (9.1 kcal mol^{–1}). Such is not the case for **BTP**→**BDP**→**BMP** pathway where the same magnitude of strain release (6.3 kcal mol^{–1}) is found for both steps. The “gradient” observed in the **BTF** series is a novel observation among reactive small-molecule systems and may help to rationalize the unusual aminolysis reactivity of the parent molecule. Future work could consider theoretically modelling the specific consecutive aminolysis reactions where the differences in transition state energies (e.g., for the putative tetrahedral intermediates) could alternatively link strain and reactivity.

Conclusions. When the unexpectedly efficient sequential aminolysis capability of benzotriuranone (**BTF**) was identified several years ago¹⁰ it both highlighted the exclusivity of cyanuric chloride (**CC**) with respect to this chemical behaviour and offered a new structural basis upon which to consider achieving selective and stepwise transformations. In this work the origins of **BTF**’s sequential reactivity profile have been more comprehensively understood through comparison of the trilactone to structurally related molecules and a combination of kinetics measurements, X-ray crystallography, and computational analysis. Revealed is that the increasingly slowed aminolysis rates as **BTF**→**1**→**2**→**3**, and the extremely fast reaction of **BTF** with amines (versus **BTP** but also conventional “activated” esters), is best rationalized through a synergy of ring strain and inductive effects. More compellingly, while ring strain is relieved upon the sequential aminolysis of both **BTF** and **BTP**, it is only in the former that a ring strain gradient is established that amplifies stepwise aminolysis rate differences and contributes to enhanced selectivity.

Singular strain release events are a powerful and much appreciated way to promote chemical reactions.¹² Beyond this, and exposed fortuitously by **BTF**, one could consider marrying electronic and strain effects in new ways to establish useful kinetic gradients and/or unprecedented levels of chemoselectivity. Along these lines, and toward the design of new molecular examples, it is exciting to see how well modern day computational methods can predict reactivity trends on the basis of readily accessible structural/electronic parameters. In

the short term we are exploring whether ring strain as it is diagnosed by the so-called Mills-Nixon effect is a useful starting point for identifying such new scaffolds for one-pot molecular multifunctionalization schemes.

EXPERIMENTAL SECTION

General Information. DMF was degassed in 20 L drums and passed through two sequential purification columns (molecular sieves) under a positive argon atmosphere. Thin layer chromatography (TLC) was performed on aluminum backed SiO₂-60 F254 TLC plates with visualization via UV light and either ninhydrin or KMnO₄ stains; products stained different colors based on the number of lactone rings present. Flash column chromatography was performed using SiO₂-60 230-400 mesh silica gel and mobile phases as indicated within procedures. ¹H NMR and ¹³C NMR were recorded on spectrometers operating at 300 or 500 MHz for ¹H and at 75 or 126 MHz for ¹³C as specified. Chemical shifts (δ) are given in parts per million (ppm) relative to residual protonated solvent (DMSO-*d*₆: δ_{H} 2.50 ppm, δ_{C} 39.50 ppm; CDCl₃: δ_{H} 7.24 ppm, δ_{C} 77.0 ppm). Abbreviations used are s (singlet), d (doublet), t (triplet), q (quartet), p (pentet), and m (multiplet). MS spectra (HRMS) were acquired on a 4.7 T Fourier Transform Ion Cyclotron Resonance mass spectrometer. EI-MS spectra were recorded on a single quadrupole spectrometer. Electrospray ionization (ESI) or Direct Analysis in Real Time (DART) high resolution mass spectra (HRMS) were recorded on an ESI-TOF instrument, operating in positive or negative ion mode as stated, with methanol as the carrier solvent for ESI experiments. The following compounds were prepared based on our earlier literature procedures and provided ¹H NMR data consistent with the literature: **1c**,¹⁰ triisopropyl 3,3',3''-(2,4,6-trihydroxybenzene-1,3,5-triyl)tripropionate,¹³ **BMF** (2-coumaranone),¹¹ and **BTF**.¹¹ **BMP** (3,4-dihydrocoumarin) was obtained commercially and used without further purification.

Starting Material Synthesis. *3,4,7,8,11,12-Hexahydro-2H-dipyran[2,3-f:2',3'-h]chromene-2,6,10-trione (BTP)*. To a solution of triisopropyl 3,3',3''-(2,4,6-trihydroxybenzene-1,3,5-triyl)tripropionate¹³ (0.40 g, 0.87 mmol) in toluene (40 mL) was slowly added trifluoroacetic acid (2 mL) under argon. The solution was then heated at 80 °C for 2 h. The orange solution was concentrated under vacuo to give **BTP** (0.25 g, quant) as an off-white solid with no further purification required: ¹H NMR (500 MHz, DMSO-*d*₆): δ 2.94 (t, *J* = 7.3 Hz, 6H), 2.79 (t, *J* = 7.3 Hz, 6H). ¹³C NMR (126 MHz, DMSO-*d*₆): δ 167.3, 147.4, 106.9, 27.6, 16.9. HRMS (EI) calcd for C₁₅H₁₂O₆ [M]⁺: 288.0634, found: 288.0659. IR (CH₃CN): $\nu_{\text{C=O}}$ 1777 cm⁻¹.

Benzene-1,3,5-triyl triacetate (4). Phloroglucinol triacetate was prepared using a general literature approach (representative procedure³⁸). NMR data, recorded in DMSO-*d*₆, is consistent with the structure of the known compound. ¹H NMR (500 MHz, DMSO-*d*₆): δ 6.94 (s, 3H), 2.26 (s, 9H). ¹³C NMR (126 MHz, DMSO-*d*₆): δ 168.7, 150.9, 113.5, 20.7. IR (CH₃CN): $\nu_{\text{C=O}}$ 1774 cm⁻¹.

Preparation of Representative/Model Compounds via Aminolysis.

N-Benzyl-3-(5-hydroxy-2,8-dioxo-2,3,4,8,9,10-hexahydropyran[2,3-f]chromen-6-yl)propanamide (5a). To a solution of **BTP** (50.0 mg, 173 μ mol) in DMF (5 mL), cooled to -41 °C, was dropwise added a benzylamine (**a**) solution (346 μ L of a 0.503 M solution in DMF, 174 μ mol). TLC analysis showed modest change after 4 h, so the reaction was allowed to warm to rt overnight, diluted with EtOAc, and washed sequentially with 0.1N HCl, DI H₂O (\times 3), then brine. The organics were dried over Na₂SO₄ and volatiles were removed in vacuo. Compound **5a** was isolated via column chromatography (acetone gradient in DCM; *R*_f ~ 0.5 in 5% acetone in DCM) to yield a colorless oil (52.0 mg, 76% yield). ¹H NMR (500 MHz, DMSO-*d*₆): δ 9.69 (s,

1H), 8.60 (t, *J* = 5.8 Hz, 1H), 7.30 (m, 2H), 7.22 (m, 3H), 4.28 (d, *J* = 5.5 Hz, 2H), 2.89–2.70 (m, 12H). ¹³C NMR (126 MHz, DMSO-*d*₆): δ 173.0, 168.0, 167.9, 151.1, 149.1, 147.1, 139.0, 128.3, 127.2, 126.8, 112.2, 107.1, 102.6, 42.3, 34.5, 28.0, 27.9, 18.3, 17.6, 16.8. HRMS (ESI) calcd (*m/z*) for C₂₂H₂₁NNaO₆ [M+Na]⁺ 418.1261, found 418.1272.

N-Heptyl-3-(5-hydroxy-2,8-dioxo-2,3,4,8,9,10-hexahydropyran[2,3-f]chromen-6-yl)propanamide (5b). To a solution of **BTP** (49.3 mg, 171 μ mol) in DMF (3 mL), cooled to -41 °C, was dropwise added an *n*-heptylamine (**b**) solution (340 μ L of a 0.503 M solution in DMF, 171 μ mol). The reaction mixture was allowed to stir for 6 h and then warmed to rt overnight, diluted with EtOAc, and washed sequentially with 0.1 N HCl, DI H₂O (\times 3), then brine. Compound **5b** was isolated after column chromatography (gradient, 0–95% EtOAc in hexanes; *R*_f ~ 0.5 in 1:1 hexanes/EtOAc) yielding an amorphous solid (44 mg, 71% yield). ¹H NMR (500 MHz, DMSO-*d*₆): δ 9.89 (s, 1H), 8.10 (t, *J* = 5.5 Hz, 1H), 3.03 (q, *J* = 6.8 Hz, 2H), 2.85 (m, 6H), 2.73 (m, 6H), 2.44 (t, *J* = 6.7 Hz, 2H), 1.36 (m, 2H), 1.21 (m, 6H), 0.85 (t, *J* = 6.8 Hz, 3H). ¹³C NMR (126 MHz, DMSO-*d*₆): δ 173.1, 168.0, 167.9, 151.2, 149.1, 147.1, 112.3, 107.1, 102.6, 38.8, 34.4, 31.2, 28.8, 28.3, 28.1, 27.9, 26.3, 22.0, 18.1, 17.6, 16.8, 13.9. HRMS (ESI) calcd (*m/z*) for C₂₂H₂₉NNaO₆ [M+Na]⁺ 426.1887, found 426.1895. IR (CH₃CN): $\nu_{\text{C=O(lactone)}}$ 1773 cm⁻¹ (two absorptions, unresolved).

3,3'-(5,7-Dihydroxy-2-oxochroman-6,8-diyl)bis(N-benzylpropanamide) (6aa). To a solution of **BTP** (50.0 mg, 174 μ mol) in DMF (3 mL), cooled to -41 °C, was dropwise added a benzylamine (**a**) solution (800.4 μ L of a 0.503 M solution in DMF, 400 μ mol). The reaction mixture was allowed to stir for 12 h before warming to rt; the reaction was worked up similar to **5a**. Compound **6aa** was isolated via column chromatography (acetone into DCM gradient, *R*_f ~ 0.5 in 10% acetone in DCM) yielding an amorphous solid (53 mg, 61% yield). ¹H NMR (300 MHz, CDCl₃): δ 9.44 (s, 1H), 9.32 (s, 1H), 7.27–7.21 (m, 6H), 7.14–7.07 (m, 4H), 6.06 (t, *J* = 5.6 Hz, 1H), 5.98 (t, *J* = 5.5 Hz, 1H), 4.36 (d, *J* = 5.7 Hz, 2H), 4.34 (d, *J* = 5.8 Hz, 2H), 2.95–2.86 (m, 6H), 2.68–2.61 (m, 6H). ¹³C NMR (CDCl₃): δ 175.2, 174.9, 169.6, 153.4, 151.6, 149.7, 137.4, 137.3, 128.8, 128.7, 127.7 (3 peaks), 113.3, 107.9, 103.5, 44.0, 35.8, 35.3, 29.2, 18.6, 17.8, 17.8 (missing two peaks). HRMS (ESI) calcd (*m/z*) for C₂₉H₃₀N₂NaO₆ [M+Na]⁺ 525.1996, found 525.2011.

3,3'-(5,7-Dihydroxy-2-oxochroman-6,8-diyl)bis(N-heptylpropanamide) (6bb). **BTP** (50.0 mg, 173 μ mol) was dissolved in DMF and cooled to 0 °C in an ice bath before dropwise addition of an *n*-heptylamine (**b**) solution (51.6 μ L, 348 μ mol). The reaction was allowed to stir overnight, slowly warming to rt. The reaction was worked up similar to **5b**. Compound **6bb** was isolated via column chromatography (3%–15% EtOAc in DCM) yielding an amorphous solid (55 mg, 61% yield). ¹H NMR (500 MHz, DMSO-*d*₆): δ 9.52 (s, 1H), 9.30 (s, 1H), 8.11 (t, *J* = 5.7 Hz, 1H), 8.04 (t, *J* = 5.5 Hz, 1H), 3.02 (m, 4H), 2.77 (t, *J* = 7.2 Hz, 2H), 2.72–2.65 (m, 6H), 2.39 (m, 4H), 1.35 (m, 4H), 1.28–1.14 (m, 16H), 0.84 (m, 6H). ¹³C NMR (126 MHz, DMSO-*d*₆): δ 173.9, 173.2, 168.7, 152.6, 150.6, 148.9, 112.8, 108.0, 102.6, 38.8, 38.7, 34.9, 34.6, 31.2, 28.9, 28.9, 28.5, 28.4, 26.3, 22.0, 18.5, 18.2, 17.6, 13.9 (missing five peaks). HRMS (ESI) calcd (*m/z*) for C₂₉H₄₇N₂O₆ [M+H]⁺ 519.3429, found 519.3439. IR (CH₃CN): $\nu_{\text{C=O(lactone)}}$ 1766 cm⁻¹.

3,3',3''-(2,4,6-Trihydroxybenzene-1,3,5-triyl)tris(N-heptylpropanamide) (7bbb). **BTP** (25.3 mg, 87.8 μ mol) was dissolved into CH₃CN (10 mL) and then *n*-heptylamine (**b**) (235 μ L, 1.58 mmol) was added dropwise. The reaction was allowed to proceed for 20 h before pouring into EtOAc and washing with 1 N HCl, DI H₂O, and brine. Organics were dried over Na₂SO₄ and volatiles were removed in vacuo. The crude was purified via

column chromatography (gradient, 0–100% EtOAc in hexanes) yielding **7bbb** an amorphous solid (54 mg, 97% yield). ¹H NMR (500 MHz, DMSO-*d*₆) δ 9.05 (s, 3H), 8.07 (t, *J* = 5.7 Hz, 3H), 3.01 (q, *J* = 6.6 Hz, 6H), 2.62 (t, *J* = 6.4 Hz, 6H), 2.38 (t, *J* = 6.3 Hz, 6H), 1.34 (p, *J* = 7.2 Hz, 6H), 1.27–1.15 (m, 24H), 0.84 (t, *J* = 6.9 Hz, 9H). ¹³C NMR (126 MHz, DMSO-*d*₆) δ 174.2, 152.1, 108.2, 38.8, 34.9, 31.2, 28.9, 28.4, 26.3, 22.0, 18.5, 13.9. HRMS (ESI) calcd for C₃₆H₆₃N₃NaO₆ [M+Na]⁺ 656.4609; found 656.4579.

N-Heptyl-2-(2-hydroxyphenyl)acetamide (*n*-heptyl aminolysis product of **BMF**). To a solution of 2-coumaranone (0.100 g, 0.746 mmol) in dry MeCN at rt under an argon atmosphere was added *n*-heptylamine (220 μL, 1.49 mmol) and the reaction was stirred for 16 h. The mixture was then dissolved in CHCl₃ (50 mL) and washed with 1 M HCl (25 mL), water (25 mL), and brine (25 mL). The organic phase was dried over Na₂SO₄, concentrated and purified by flash chromatography using EtOAc/hexanes 30% to afford the product (0.699 mmol, 94% yield) as a white solid: ¹H NMR (500 MHz, DMSO-*d*₆) δ 9.75 (s, 1H), 7.97 (t, *J* = 5.2 Hz, 1H), 7.08–7.01 (m, 2H), 6.78 (d, *J* = 8.4 Hz, 1H), 6.72 (t, *J* = 7.4 Hz, 1H), 3.38 (s, 2H), 3.04 (q, *J* = 6.8 Hz, 2H), 1.40 (p, *J* = 6.7 Hz, 2H), 1.31–1.17 (m, 8H), 0.85 (t, *J* = 6.8 Hz, 3H). ¹³C NMR (126 MHz, DMSO-*d*₆) δ 170.9, 155.5, 130.5, 127.6, 122.7, 118.9, 115.4, 38.7, 37.5, 31.2, 29.0, 28.4, 26.3, 22.0, 13.9. HRMS (ESI) calcd for C₁₅H₂₃NO₂ [M + Na]⁺ 272.1621; found 272.1624.

N-Heptyl-3-(2-hydroxyphenyl)propanamide (*n*-heptyl aminolysis product of **BMP**). To a solution of dihydrocoumarin (95 μL, 0.746 mmol) in dry MeCN at rt under an argon atmosphere was added *n*-heptylamine (220 μL, 1.49 mmol) and the reaction was stirred for 16 h. The mixture was then dissolved in CHCl₃ (50 mL) and washed with 1 M HCl (25 mL), water (25 mL), and brine (25 mL). The organic phase was dried over Na₂SO₄, concentrated and purified by flash chromatography using EtOAc/hexanes 30% to afford the product (0.711 mmol, 95% yield) as a white solid: ¹H NMR (500 MHz, DMSO-*d*₆) δ 9.28 (s, 1H), 7.75 (t, *J* = 5.3 Hz, 1H), 7.02 (d, *J* = 7.8 Hz, 9H), 6.98 (t, *J* = 8.3 Hz, 1H), 6.75 (d, *J* = 7.9 Hz, 1H), 6.68 (t, *J* = 7.4 Hz, 1H), 3.01 (q, *J* = 6.7 Hz, 2H), 2.71 (t, *J* = 7.7 Hz, 2H), 2.31 (d, *J* = 7.9 Hz, 3H), 1.35 (p, *J* = 7.0 Hz, 2H), 1.31–1.15 (m, 8H), 0.86 (t, *J* = 6.9 Hz, 3H). ¹³C NMR (126 MHz, DMSO-*d*₆) δ 171.6, 155.0, 129.6, 127.5, 126.9, 118.8, 114.9, 38.4, 35.4, 31.2, 29.1, 28.4, 26.3, 25.7, 22.0, 13.9. HRMS (ESI) calcd for C₁₆H₂₅NO₂ [M + Na]⁺ 286.1778; found 286.1792.

5-Hydroxy-1,3-phenylene diacetate (*by*-product of *n*-heptyl aminolysis of **4**). Benzene-1,3,5-triyl triacetate **4** (0.977 g, 3.87 mmol) and DMF (50 mL) were cooled to –40 °C before dropwise addition of *n*-heptylamine (**b**) (576 μL, 3.87 mmol). The reaction mixture was allowed to slowly warm to rt over 6 h. The reaction mixture was then poured into EtOAc and washed extensively with DI H₂O followed by brine. The organics were dried over Na₂SO₄ and the volatiles were removed in vacuo yielding a crude oil. The crude mixture was purified via column chromatography (40% EtOAc in hexanes; *R*_f ~ 0.4) to yield the aminolysis product (480 mg, 60%) as a white solid. The NMR data is consistent with the literature.³⁹ ¹H NMR (500 MHz, DMSO-*d*₆): δ 10.02 (s, 1H), 6.43 (d, 2H, *J* = 2.0 Hz), 6.38 (t, 1H, *J* = 2.0 Hz), 2.23 (s, 6H). ¹³C NMR (126 MHz, DMSO-*d*₆) δ 168.8, 158.5, 151.4, 106.6, 106.4, 20.8. IR (CH₃CN): ν_{C=O} 1768 cm⁻¹.

3,5-Dihydroxyphenyl acetate (*by*-product of *n*-heptyl aminolysis of **4**). Prepared for verification using a general phloroglucinol acetylation procedure provided in the literature.³⁹ To phloroglucinol (500 mg, 3.96 mmol) in pyridine (10 mL) was added acetic anhydride (445 mg, 4.36 mmol) and the reaction mixture was allowed to reflux for 3 h before cooling to rt. The solvent was removed in vacuo and the residue was purified via column chromatography (1:1 EtOAc:hexanes). After removal of volatiles, a clear oil was obtained (500 mg, 75%). NMR data, recorded in DMSO-*d*₆, is consistent with the structure of the compound.⁴⁰ ¹H

NMR (500 MHz, DMSO-*d*₆): δ 9.47 (s, 2H), 6.09 (t, 1H, *J* = 2.0 Hz), 5.94 (d, 2H, *J* = 2.0 Hz), 2.19 (s, 3H) (peak at 2.08 ppm is CH₃CN). ¹³C NMR (126 MHz, DMSO-*d*₆) δ 168.9, 158.7, 151.9, 100.1, 99.9, 20.9. IR (CH₃CN): ν_{C=O} 1764 cm⁻¹.

Aminolysis Kinetics. Kinetics of the aminolysis of **BTF**, **BTP**, **BMF**, **BMP**, **1b**, **2bb**, **4**, **5b**, **6bb**, at 24.0 ± 0.2 °C in acetonitrile was followed as described above on an infrared spectrophotometer coupled with a stopped-flow injection system and equipped with a 100 μm path length stopped flow cell. In general, at least a 15-fold excess of *n*-heptylamine was used for each run. Each average *k*_{obs} was determined as the average of 3–6 independent runs. Concentrations of compound were determined utilizing a microbalance and volumetric flasks. See the Supporting Information for additional details.

ASSOCIATED CONTENT

Supporting Information. NMR data, aminolysis kinetics data and mathematical predictions, computational details (including energies and coordinates of geometry-minimized structures), and details of X-ray data collection and structure refinement (PDF). This material is available free of charge via the Internet at <http://pubs.acs.org>.

AUTHOR INFORMATION

Corresponding Author

*E-mail: castellano@chem.ufl.edu.

Present Address

†MERLN Institute for Technology-Inspired Regenerative Medicine, Maastricht University, PO Box 616, 6200 MD Maastricht, The Netherlands.

ACKNOWLEDGMENTS

Acknowledgement is made to the donors of the American Chemical Society Petroleum Research Fund (PRF # 51880-ND4) and the University of Florida (graduate fellowships to M.B.B., R.B.F., and A.J.L.) for support of this research. Additional support for A.A. is acknowledged from the National Science Foundation REU program (CHE-0353828). The authors are grateful to the University of Florida High-Performance Computing Center for providing computational resources and both the University of Florida and the National Science Foundation (CHE-0821346) for funding the X-ray equipment. We would finally like to thank Prof. Leslie Murray for stopped-flow IR training and insightful advice and Daan van der Zwaag for assistance in the mathematical analysis of the reaction kinetics.

REFERENCES

- (a) Lee, J.-S.; Lee, J. W.; Kang, N.; Ha, H.-H.; Chang, Y.-T., *Chem. Rec.* **2015**, *15*, 495–510; (b) Vaxelaire, C.; Winter, P.; Christmann, M., *Angew. Chem. Int. Ed.* **2011**, *50*, 3605–3607.
- Brauch, S.; van Berkel, S. S.; Westermann, B., *Chem. Soc. Rev.* **2013**, *42*, 4948–4962.
- Fries, H. H., *J. Chem. Soc., Trans.* **1886**, *49*, 314–316.
- Cuthbertson, W. W.; Moffatt, J. S., *J. Chem. Soc. (Resumed)* **1948**, 561–564.
- (a) Jagadeesh Kumar, G.; Sriramkumar Bomma, H. V. S.; Srihari, E.; Shrivastava, S.; Naidu, V. G. M.; Srinivas, K.; Jayathirtha Rao, V., *Med. Chem. Res.* **2013**, *22*, 5973–5981; (b) Banerjee, R.; Brown, D. R.; Weerapana, E., *Synlett* **2013**, *24*, 1599–1605; (c) Lim, J.; Simanek, E. E., *Adv. Drug Delivery Rev.* **2012**, *64*, 826–835.
- Gamez, P.; Reedijk, J., *Eur. J. Inorg. Chem.* **2006**, *2006*, 29–42.
- Blotny, G., *Tetrahedron* **2006**, *62*, 9507–9522.
- (a) Kubo, T.; Figg, C. A.; Swartz, J. L.; Brooks, W. L. A.; Sumerlin, B. S., *Macromolecules* **2016**, *49*, 2077–2084; (b) Figg, C. A.; Kubo, T.; Sumerlin, B. S., *ACS Macro Lett.* **2015**, *4*, 1114–1118.

- (9) Ramesh, A.; Syama Sundar, B.; Radhakrishna Murti, P. S., *J. Indian Chem. Soc.* **1995**, *72*, 697–700.
- (10) Baker, M. B.; Ghiviriga, I.; Castellano, R. K., *Chem. Sci.* **2012**, *3*, 1095–1099.
- (11) Li, Y.; Lampkins, A. J.; Baker, M. B.; Sumpster, B. G.; Huang, J.; Abboud, K. A.; Castellano, R. K., *Org. Lett.* **2009**, *11*, 4314–4317.
- (12) (a) Wilson, M. R.; Taylor, R. E., *Angew. Chem. Int. Ed.* **2013**, *52*, 4078–4087; (b) Gold, B.; Dudley, G. B.; Alabugin, I. V., *J. Am. Chem. Soc.* **2013**, *135*, 1558–1569; (c) Agard, N. J.; Prescher, J. A.; Bertozzi, C. R., *J. Am. Chem. Soc.* **2004**, *126*, 15046–15047; (d) Stirling, C. J. M., *Tetrahedron* **1985**, *41*, 1613–1666.
- (13) Lampkins, A. J.; Li, Y.; Al Abbas, A.; Abboud, K. A.; Ghiviriga, I.; Castellano, R. K., *Chem. Eur. J.* **2008**, *14*, 1452–1463.
- (14) (a) Um, I.-H.; Bae, A. R., *J. Org. Chem.* **2011**, *76*, 7510–7515; (b) Galabov, B.; Ilieva, S.; Hadjieva, B.; Atanasov, Y.; Schaefer, H. F., *J. Phys. Chem. A* **2008**, *112*, 6700–6707; (c) Um, I.-H.; Jeon, S.-E.; Seok, J.-A., *Chem. Eur. J.* **2006**, *12*, 1237–1243; (d) Neuvonen, H.; Neuvonen, K.; Koch, A.; Kleinpeter, E.; Pasanen, P., *J. Org. Chem.* **2002**, *67*, 6995–7003; (e) Koh, H. J.; Kim, S. I.; Lee, B. C.; Lee, I., *J. Chem. Soc., Perkin Trans. 2* **1996**, 1353–1357; (f) Menger, F. M.; Smith, J. H., *J. Am. Chem. Soc.* **1972**, *94*, 3824–3829.
- (15) (a) Yi, G.-Q.; Zeng, Y.; Xia, X.-F.; Xue, Y.; Kim, C.-K.; Yan, G.-S., *Chem. Phys.* **2008**, *345*, 73–81; (b) Sung, D. D.; Koo, I. S.; Yang, K.; Lee, I., *Chem. Phys. Lett.* **2006**, *426*, 280–284.
- (16) Maude, A. B.; Williams, A., *J. Chem. Soc., Perkin Trans. 2* **1997**, 179–184.
- (17) Izbiccka, E.; Bolen, D. W., *J. Am. Chem. Soc.* **1978**, *100*, 7625–7628.
- (18) (a) Svirbely, W. J.; Blauer, J. A., *J. Am. Chem. Soc.* **1961**, *83*, 4115–4118; (b) Svirbely, W. J., *J. Am. Chem. Soc.* **1959**, *81*, 255–257; (c) Svirbely, W. J., *J. Phys. Chem.* **1958**, *62*, 380–380.
- (19) Friedman, M. H.; White, R. R., *AIChE J.* **1962**, *8*, 581–586.
- (20) Haines, A. H.; Hughes, D. L., *Acta Crystallogr., Sect. E: Crystallogr. Commun.* **2009**, *65*, o3279.
- (21) While the protonation state of the products and reactants (i.e., –OH vs. –O–) have not been measured under the reaction conditions, significant deprotonation is not expected given the difference in pK_a between phloroglucinol (estimated; 20–25) and *n*-butylammonium (18.3) in acetonitrile. See Kütt, A.; Leito, I.; Kaljurand, I.; Sooväli, L.; Vlasov, V. M.; Yagupolskii, L. M.; Koppel, I. A., *J. Org. Chem.* **2006**, *71*, 2829–2838 for molecules serving as the basis of the pK_a estimation.
- (22) Hansch, C.; Leo, A.; Taft, R. W., *Chem. Rev.* **1991**, *91*, 165–195.
- (23) (a) Neuvonen, H.; Neuvonen, K., *J. Chem. Soc., Perkin Trans. 2* **1999**, 1497–1502; (b) Bromilow, J.; Brownlee, R. T. C.; Craik, D. J.; Fiske, P. R.; Rowe, J. E.; Sadek, M., *J. Chem. Soc., Perkin Trans. 2* **1981**, 753–759.
- (24) Um, I.-H.; Lee, J.-Y.; Fujio, M.; Tsuno, Y., *Org. Biomol. Chem.* **2006**, *4*, 2979–2985.
- (25) Neuvonen, H.; Neuvonen, K.; Koch, A.; Kleinpeter, E., *J. Phys. Chem. A* **2005**, *109*, 6279–6289.
- (26) Reed, A. E.; Curtiss, L. A.; Weinhold, F., *Chem. Rev.* **1988**, *88*, 899–926.
- (27) (a) Chattaraj, P. K.; Sarkar, U.; Roy, D. R., *Chem. Rev.* **2006**, *106*, 2065–2091; (b) Parr, R. G.; Szentpály, L. v.; Liu, S., *J. Am. Chem. Soc.* **1999**, *121*, 1922–1924.
- (28) (a) Galabov, B.; Ilieva, S.; Schaefer, H. F., *J. Org. Chem.* **2006**, *71*, 6382–6387; (b) Kollman, P.; McKelvey, J.; Johansson, A.; Rothenberg, S., *J. Am. Chem. Soc.* **1975**, *97*, 955–965.
- (29) Shaik, S.; Shurki, A.; Danovich, D.; Hiberty, P. C., *Chem. Rev.* **2001**, *101*, 1501–1540.
- (30) Boese, R.; Bläser, D.; Billups, W. E.; Haley, M. M.; Maulitz, A. H.; Mohler, D. L.; Vollhardt, K. P. C., *Angew. Chem. Int. Ed.* **1994**, *33*, 313–317.
- (31) (a) Stanger, A., *Chem. Commun.* **2009**, 1939–1947; (b) Bürgi, H.-B.; Baldrige, K. K.; Hardcastle, K.; Frank, N. L.; Gantzel, P.; Siegel, J. S.; Ziller, J., *Angew. Chem. Int. Ed.* **1995**, *34*, 1454–1456; (c) Siegel, J. S., *Angew. Chem. Int. Ed.* **1994**, *33*, 1721–1723.
- (32) Hall, H. K.; Zbinden, R., *J. Am. Chem. Soc.* **1958**, *80*, 6428–6432.
- (33) Leitão, M. L. P.; Pilcher, G.; Meng-Yan, Y.; Brown, J. M.; Conn, A. D., *J. Chem. Thermodyn.* **1990**, *22*, 885–891.
- (34) (a) Houk, K. N.; Jabbari, A.; Hall, H. K.; Alemán, C., *J. Org. Chem.* **2008**, *73*, 2674–2678; (b) Brown, H. C.; Brewster, J. H.; Shechter, H., *J. Am. Chem. Soc.* **1954**, *76*, 467–474; (c) Carothers, W. H.; Dorough, G. L.; Natta, F. J. v., *J. Am. Chem. Soc.* **1932**, *54*, 761–772.
- (35) Sousa, C. C. S.; Matos, M. A. R.; Santos, L. M. N. B. F.; Morais, V. M. F., *J. Chem. Thermodyn.* **2013**, *67*, 210–216.
- (36) Matos, M. A. R.; Sousa, C. C. S.; Morais, V. M. F., *J. Chem. Thermodyn.* **2009**, *41*, 308–314.
- (37) Wheeler, S. E.; Houk, K. N.; Schleyer, P. v. R.; Allen, W. D., *J. Am. Chem. Soc.* **2009**, *131*, 2547–2560.
- (38) Bazin, M.-A.; Boderio, L.; Tomasoni, C.; Rousseau, B.; Roussakis, C.; Marchand, P., *Eur. J. Med. Chem.* **2013**, *69*, 823–832.
- (39) Sapkota, K.; Roh, E.; Lee, E.; Ha, E.-M.; Yang, J.-H.; Lee, E.-S.; Kwon, Y.; Kim, Y.; Na, Y., *Bioorg. Med. Chem.* **2011**, *19*, 2168–2175.
- (40) Carnduff, J.; Miller, J. A.; Stockdale, B. R.; Larkin, J.; Nonhebel, D. C.; Wood, H. C. S., *J. Chem. Soc., Perkin Trans. 1* **1972**, 692–699.

Table of Contents/Abstract Graphic

